

2.4 GHZ WIRELESS ELECTROMYOGRAPH SYSTEM WITH STATISTICALLY OPTIMAL AUTOMATIC GAIN CONTROL

Design and Performance Analysis

Andrea Morici, Giorgio Biagetti and Claudio Turchetti
*DIBET — Dipartimento di Ingegneria Biomedica, Elettronica e Telecomunicazioni
Università Politecnica delle Marche, I-60131 Ancona, Italy*

Keywords: Wireless sensors, Surface EMG, IEEE 802.15.4, LR-WPAN, AGC, Laplacian distribution.

Abstract: In this paper a wireless system for *non-invasive surface electromyography* (SEMG) is presented. The use of a wireless technology, that substitutes cabled electrodes with a wireless link, allows the number of sensors on the body to be increased without affecting the patient's freedom of movement. Problems in this setup, that extend from energy consumption minimization, to satisfaction of wireless link operational bandwidth and distance requirements, and from the necessity of embedding hardware in an appreciably small device, to making it not too expensive to final customers, have been deeply analyzed and solved. In this context, low rate wireless personal area networks (LR-WPANs) proved to be a good choice for the realization of low-cost embedded wireless electrodes for electromyography. Following these considerations, a low-cost electromyographical wireless device, based on an off-the-shelf IEEE 802.15.4-compatible RF transceiver, have been designed and realized, and optimized signal processing algorithms developed to enhance the system accuracy. In particular, due to the wide range of possible amplitudes for the SEMG signal, an optimal automatic gain control, based on a detailed statistical signal analysis, have been developed to reduce the distortion at the output of the quantizer.

1 INTRODUCTION

Electromyography (EMG) is a useful diagnosis technique in the field of neurophysiology, used for evaluating and recording physiologic properties of muscles both at rest and while contracting. EMG can either use needle electrodes (intramuscular EMG) or surface electrodes (surface EMG) (Berzuini et al., 1985). Naturally, only the latter is a non-invasive technique, and is the one with which we deal in this paper.

The prediction of muscle force from EMG (Staudenmann et al., 2006) may aid with the diagnosis of some medical conditions in which the electrical activity of the muscles or nerves is not normal, such as nerve compression or injury, nerve root injury, and with other possibly muscle-related problems such as deambulation difficulties. This technique is not only useful in hospital environments, but also in rehabilitation and motion analysis laboratories, as well as in fitness centers, as it provides an assessment of the electrical activity generated by contracting muscles during movements (Jansen et al., 2003). Today the non-invasive Surface Electromyography (SEMG) has

become very popular owing to the great variety of applications it can be used in. Recently, to mention just few examples, EMG has proven to be useful as a sensor for measuring everyday playing behaviour of children (Kawakami et al., 2007), as an interface for inputting characters to a computer (Miyazawa et al., 2006) and for studies of gait dynamics in free-running insects (Lemmerhirt et al., 2006).

A typical SEMG analysis may exercise multiple sensors positioned on the patient's body, each of which may require one or more data channels. A wireless recorder system is thus demanded so that the patient's freedom of mobility does not decrease with the number of sensors applied. Some issues that an SEMG recorder system must face are related to its input sensitivity, as it is well established that the amplitude of the EMG signal ranges from 0 to 10 mV (peak-to-peak) or 0 to 1.5 mV (rms) and that is contaminated by several sources of noise, thus a high-gain differential amplifier with a CMRR of at least 80 dB is required. Other problems are related to the number of channels to be acquired: successful analysis of motion activity involving a group of muscles

needs a multiple channel recording, able to evaluate more than one EMG channel simultaneously. In this paper a multi-channel SEMG recorder system, consisting of a wireless wearable sensor interfaced to a standard PC for back-end data analysis, has been developed to satisfy the requirements of portability, high sensitivity and low-cost.

The research objectives of this article is to propose a new design of an embedded system made with off-the-shelf components and suitable for the above purposes. A statistical analysis of the EMG signal is provided and exploited to optimize the algorithms, used to enhance the performance of the low-cost components employed in the system, to levels adequate for the application. This is done by means of statistically optimized gain adjustment system that is able to achieve a better SNR respect to fixed-gain implementations.

2 ELECTROMYOGRAPHIC SIGNALS

A brief introduction on the EMG signals is necessary before presenting the hardware structure of the system. The source of EMG signal is the electrical potential generated by muscle cells when they contract. Using a surface electrode, only the general picture of muscle activation is monitored, whereas the activity of just a few fibers can be observed using needle electrodes. The amplitude of the resulting signal can range from less than 50 μV to about 5 mV. As the usable energy of the signal is limited to the 0 to 500 Hz frequency range, with the dominant energy being in the 50 to 150 Hz range, the sampling frequencies needed for its acquisition are in the order of kilohertz, generally from 1 kHz upwards. In order to get EMG voltage signals, a differential pair of Ag/AgCl electrodes is commonly used. These will pick up the voltage difference and through two very short shielded conductors it will be fed to an instrumentation amplifier on the acquisition device, that adjusts the amplitude of the EMG signal to an appropriate range for the analog to digital converter (ADC) as will be shown next.

An example of a typical EMG signal is shown in Figure 1, which reports its time progress as acquired by our system at a sample rate of 2 kHz.

The periods where the signal amplitude is low and flat correspond to the muscle being at rest, and the recorded signal is dominated by electrical noise from both the environment and the acquisition system. The parts in which the amplitude is increased above such noise floor correspond to muscle contractions. The

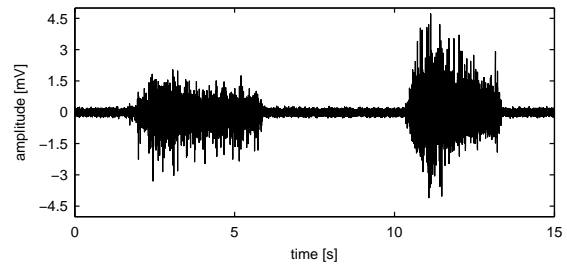


Figure 1: EMG signal recorded on a biceps muscle with the presented system.

subject of the acquisition is a biceps humerus muscle of a young adult male who was asked to perform repeated liftings of his arm following a randomised sequence. Some contractions have been kept for several seconds. The exercise was executed in a non stressed condition.

2.1 Statistical Analysis for Optimal Automatic Gain Control

A detailed knowledge of the statistical EMG signal amplitude is necessary to devise optimum strategies to properly amplify the EMG signals before feeding them to the quantizer used for the analog to digital conversion, since for proper evaluation of muscle activity it is of utmost importance that the possibility of saturation is kept to a minimum, while not degrading the signal too much due to quantization.

To analyze the statistical properties of an EMG signal it is necessary to separate the two main parts previously mentioned: rest condition and activation. The former is primarily dominated by the noise generated by the electrical devices in the acquisition board, and by their susceptibility to irradiated emissions. Indeed, it can easily be verified that it is white noise with a Gaussian probability density function (PDF). The latter part consists in the recording of the overall effect of the activation potentials during the muscle contraction. Figure 2 shows an estimate of the PDF of the recorded signal cleared of the noise-only portions. Confirming already known findings (Clancy and Hogan, 1999), the EMG signal, let us call it $x(t)$, displays a Laplacian PDF, defined as

$$f_x(x) = \frac{1}{2b} \exp\left(-\frac{|x-\mu|}{b}\right) \quad (1)$$

where μ is the mean value, supposedly zero, and b is the mean absolute value (MAV), that is, $b = E\{|x|\}$, and is usually one of the most important features to be extracted from the EMG signal.

For reference, Figure 3 reports the same experimentally-obtained distribution plotted against

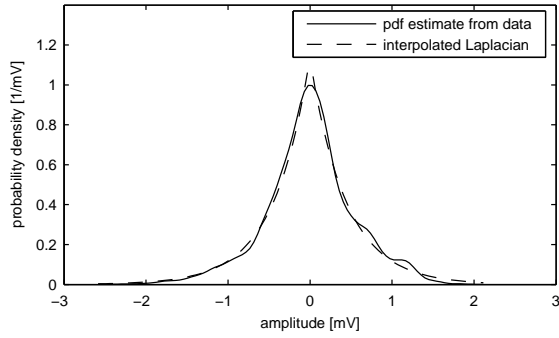


Figure 2: Probability density function of the EMG signal of Fig. 1 compared to its best fitting Laplacian distribution.

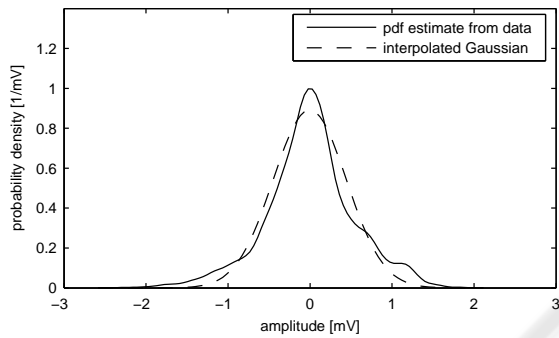


Figure 3: Probability density function of the EMG signal of Fig. 1 compared to its best fitting Gaussian distribution.

the best-fitting Gaussian distribution. There is a clear mismatch between the two, confirming that the Laplacian better describes the EMG signal statistics.

From a statistical point of view, as the non-linearity affects the signal amplitude, an optimal automatic gain control (AGC) must be able to minimize the distortion at the output of the quantizer.

Let us then suppose that the quantizer has a saturation level L , and that in between it performs the ideal staircase quantization described by

$$y = \begin{cases} \lfloor x + 1/2 \rfloor & |x| < L \\ L \operatorname{sign}(x) & |x| \geq L \end{cases} \quad (2)$$

then, the expected MAV at the quantizer's output is

$$E\{y\} = \frac{1}{b} \int_0^{L+1/2} \lfloor x + 1/2 \rfloor e^{-x/b} dx + \frac{1}{b} \int_{L+1/2}^{+\infty} L e^{-x/b} dx \quad (3)$$

where the second term at the right hand side is the contribution due to saturation effects. The first integral can easily be evaluated as follows

$$\int_0^{L+1/2} \lfloor x + 1/2 \rfloor e^{-x/b} dx = \sum_{n=1}^L \int_{n-1/2}^{n+1/2} n e^{-x/b} dx \quad (4)$$

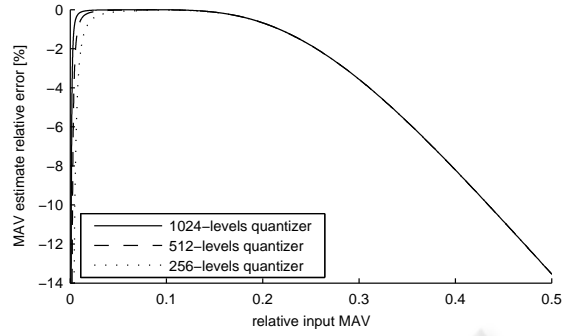


Figure 4: Error of MAV estimate after quantization and saturation as a function of input MAV (relative to full scale) for different quantizer resolutions.

which, after a few simple manipulations, yields

$$E\{y\} = \frac{1 - e^{-L/b}}{e^{1/(2b)} - e^{-1/(2b)}} \quad (5)$$

Ideally, we would like to operate the quantizer with an input signal whose amplitude b is such that its post-quantization estimate $E\{y\}$ is as close as possible to b . A measure of the error introduced by the quantizer is the relative MAV error $(E\{y\} - b)/b$, shown in Figure 4 for different quantizer resolutions as a function of the relative input signal amplitude b/L . As can be seen from the graphs, if the input level is kept close to about $0.1L$ with a proper AGC mechanism, which will be described in a following section, even low resolution quantizers can give extremely good results.

3 WIRELESS SENSOR NODE

The wireless node we propose comprise all the electronics needed to measure the biological parameters of interest, processing them both prior and after their conversion to the digital domain, and to transfer them through a wireless link to a nearby observation station. All wireless board components were chosen keeping in mind energy saving, low-cost, high integration and good electrical property, for the analog parts, consistently to EMG signal requirements.

Figure 5 shows the block diagram of our wireless node, while Figure 6 shows a photo of a prototype of the wireless embedded board for electromyography.

The sensor, that was designed to be of peel-and-stick type, detects at the skin surface a differential voltage signal that is amplified by a low-noise differential amplifier and low-pass filtered in the band of interest. This is a solution known as "active electrode," for the differential amplifier is placed as close as possible to the detection surface of the electrodes,

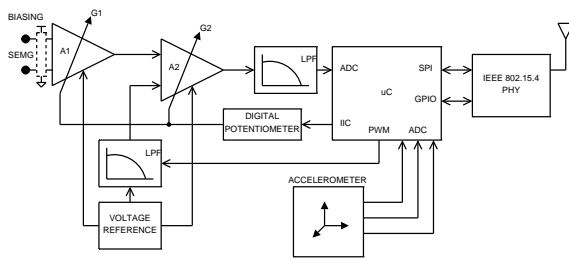


Figure 5: Block scheme of the wireless electromyograph node.

so as to improve the immunity to the noise induced by external radiated interferences. The signal, so amplified, is fed through an RC anti-imaging low-pass filter that limits the upper bound of the frequency spectrum to be acquired. Its cut-off frequency was chosen to be approximately 530 Hz.

The active sensor prototype used a two chip solution for the microcontroller part and for the wireless physical (PHY) transceiver, to facilitate laboratory testing and debugging, but in future realizations it will more convenient to switch to Platform-in-Package (PiP) solutions, where the above mentioned two chips are integrated into one package, in order to save cost, space, and PCB design difficulties.

The board also comprise the off-chip RF part, including PCB traces designed for impedance matching and discrete components chosen to achieve good impedance matching between the PHY transceiver and the chip antenna. This kind of antenna was chosen because of its small size and characteristics optimized for our operating wireless band.

The node also includes a three-axis accelerometer that can provide useful data for motion analysis when combined to EMG measurements. Moreover, it provides three additional data channels to demonstrate the bandwidth capacity in streaming four simultaneous real-time channels from the sensor node.

Acceleration data can also be an efficient way to give commands to the board, for instance to enable low power operation modes by putting the electronic devices of the board in standby during inactivity periods.

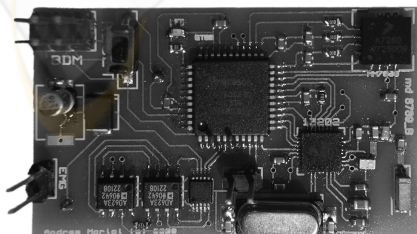


Figure 6: The wireless electromyograph embedded board. Actual size is 50 mm × 30 mm.

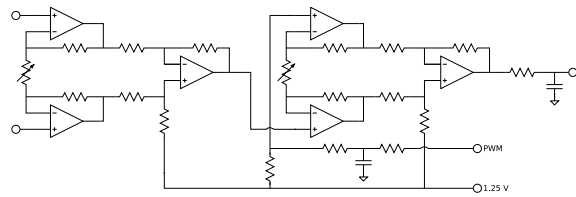


Figure 7: Details of the instrumentation amplifier configuration used.

3.1 Signal Acquisition and Conditioning

The analog signal chain for the EMG signal requires special attention. Because of the wide range in which EMG signals can vary, a cascade of two variable gain instrumentation amplifiers was used. A detailed schematic diagram of their connection is shown in Figure 7.

These amplifiers are also capable of converting the differential EMG signal to single ended, with a high CMRR, and although the circuit was optimized for operation with a gain close to 1000 (60 dB), by varying both gains it is possible to change the overall gain by ± 40 dB to accommodate very different and possibly extreme application conditions.

Indeed, the algorithm in the sensor can choose gains appropriate to different condition of use: for example, if you are walking, sensor board will have to set sensitivity parameters to adequate values to sense low level excitation potentials. On the contrary, during sport trainings muscles are probably more stressed, and so the sensor node can adjust gain parameters to achieve best measuring performance.

A dual digital potentiometer serves to make the gain variable, changing between a set of 256 different values of resistance for each stage. This level of precision is very useful when the node is moved between different muscle masses that need different gain levels, and allows for the fine-grained AGC that ensures optimal quantization.

The analog signal so amplified is subsequently converted to a digital signal by the ADC included in the microcontroller, operating at a 2 kHz sampling rate and with a maximum resolution of 10 bits.

To provide a voltage bias to the output of the amplifiers, an integrated low-cost, band-gap reference was used. The resistance seen between the output terminal of the band-gap reference and ground is only a fraction of an ohm, ensuring that the amplifier intrinsic insensitivity to common-mode voltages is not reduced because of it. With a high-CMRR input stage and a small battery-powered sensor node mounted close to the patient's skin, so as to minimize stray capacitance to ground, the use of a reference electrode

to set the patient's body potential was deemed unnecessary. Proper biasing of the input stage is provided directly to the main electrodes by means of a resistive network connected to the internal reference potential.

Despite all these precautions, it is still possible that the detected signal presents a DC component, or an input bias, high enough to cause saturation of some amplifier. To avert this possibility the circuit employs an active bias control, fed between the two amplifying stages by means of a PWM signal, that is able to cancel both amplifier bias and (small) DC components that can arise when the patient moves other parts of their body.

This active offset compensation technique was deemed to be superior to simple AC coupling, for it can use more complex filters. Moreover, since the communication channel between the node and the base station is bidirectional, these filters can be run on the PC side and thus there are potentially no limits to their complexity. For instance, we made use of fourth-order elliptical digital filters running on the PC side, with their group delay properly compensated in the reported plots. Such a solution proved to be very good at removing the spikes, usually due to patient's motion, commonly found in EMG traces, but would have been much more costly to implement in hardware.

3.2 AGC Algorithm

AGC poses a different problem than offset and bias compensation, since the latter are usually slowly time-varying phenomena for which the round-trip delay, due to the communication with the base station system, does not cause harmful degradation of the control loop stability and performance. On the contrary, the EMG signal can have quite abrupt transients. As a consequence, a simple but yet effective AGC algorithm was devised, so that it could be run on the wireless node to offer the quickest possible response time.

As previously stated, the purpose of the AGC is to keep the input MAV level to the quantizer as close as possible to $0.1L$, where L is the ADC saturation level. To this end, an estimation $\tilde{b}(t)$ of the MAV is computed with a first-order recursive digital filter,

$$\tilde{b}(t) = (1 - \alpha)\tilde{b}(t-1) + \alpha|z(t)/g(t)| \quad (6)$$

with $z(t)$ being the ADC output, $g(t)$ the amplifier gain, and α controls the filter bandwidth. Good results have been obtained with $\alpha \approx 1/64$, which corresponds to a cut-off frequency of about 5 Hz.

The optimum gain is then calculated as

$$\tilde{g}(t+1) = \frac{0.1L}{\tilde{b}(t)} \quad (7)$$

from which the actual gain $g(t+1)$ to be used next is chosen among the available gains, in steps of approximately 2 dB, with the help of a 22-entry look-up table.

3.3 Wireless Data Transmission

LR-WPAN are emerging technologies for medium distance low data rate communications. A protocol to manage this kind of networks has been defined by IEEE 802.15.4, which describes both a MAC layer and a PHY layer. The operating frequencies of the wireless link can be 868 MHz, 915 MHz or 2.4 GHz, for an available data rate respectively of 20 kbps, 40 kbps and 250 kbps. Our active sensor operates at 2.45 GHz in the ISM band to achieve maximum throughput. In this band there are 16 channels, each 5 MHz wide. Typical distances covered by this technology ranges from 30 m to 70 m in open spaces. It can be easily extended by the use of an RF power amplifier joined to an LNA. Typically they are the same as for other ISM wireless technologies such as Bluetooth and Wi-Fi. In customized applications IEEE 802.15.4 could imply difficulties in respecting timing constraints posed by real-time streaming of data, such as the one we need to perform in this context. We hence decided to only use the capabilities of the PHY layer of IEEE 802.15.4, customizing the MAC layer to our purposes. A number of active SEMG sensors, depending on how many data channels each uses, can communicate to the base station (BS) in a star topology on the same RF channel, using a custom beamed time-division multiple access (TDMA) MAC scheme. The BS is itself composed by an IEEE 802.15.4 compliant transceiver and its task is to make data available to the PC by the use of a USB link. For streaming data from multiple sensors and for achieving full-duplex operation it is necessary to assign time slots to each sensor and to transmit/receive transactions. Transmission and reception has to be scheduled by devising an adequate timing of the active sensor considering the strict requirements of the ADC sampling time. The adopted transceivers have particular timings regarding the transmission over the air of a data packet. There is a warmup period $t_{\text{warmup}} = 144 \mu\text{s}$ before the effective bitstream can be relayed, followed by a $t_{\text{cooldown}} = 10 \mu\text{s}$ cooldown period. Timings are then coherent with those reported in Figures 8 and 10:

$$t_{\text{pkt}}(B) = t_{\text{warmup}} + t_{\text{header}} + B \cdot t_{\text{byte}} + t_{\text{trailer}} + t_{\text{cooldown}} \quad (8)$$

$$t_{\text{tx}} \approx t_{\text{pkt}}(B) \Big|_{B=B_{\text{tx}}} \quad (9)$$

with $t_{\text{byte}} = 32 \mu\text{s}$ as per IEEE 802.15.4 specifications, and where the payload length B_{tx} is comprised of the EMG data bytes B_{EMG} and of the acceleration data

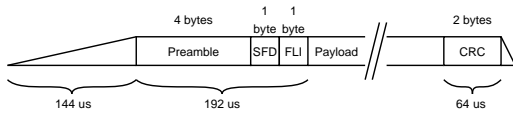


Figure 8: PHY packet transmission timings.

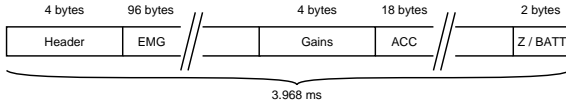


Figure 9: Packet payload content.

bytes B_{ACC} , apart from side channels (e.g. gain levels) and node status information, as shown in Fig. 9. Packet length must be chosen as a compromise between latency and channel bandwidth utilisation, as shown below.

Let us call t_{adc} the time needed by the ADC to fill B_i bytes of the payload, for the EMG and each of the three accelerometer channels:

$$t_{adc} = \frac{B_i}{N_s \cdot n_i} \cdot \frac{1}{F_{s(i)}} \quad (10)$$

where N_s is the number of bytes per sample, n_i the number of channels per sensor type in each node, sampled at a sample rate $F_{s(i)}$ (usually $n_{EMG} = 1$ for the single EMG channel sampled at $F_{s(EMG)} = 2$ kHz, and $n_{ACC} = 3$ for the three accelerometer channels sampled at a much lower sample rate $F_{s(ACC)} = 125$ Hz). Then we have the constraint

$$t_{rx} > t_{pkt}(B) \Big|_{B=B_{rx}}, \quad t_{rx} = t_{adc} - m \cdot t_{tx} \quad (11)$$

where B_{rx} is the number of bytes needed for the control channel, and m is the maximum number of wireless nodes simultaneously active.

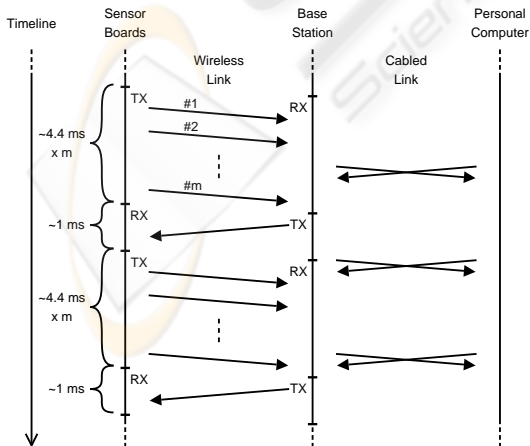


Figure 10: Communication flow scheduling of the various system components.

Table 1: Relative mean square error of the post-quantizer MAV estimate, for different quantizer resolutions, and for either a fixed gain of 60 dB and for AGC-determined gains.

| gain policy | 8 bit | 9 bit | 10 bit |
|-------------|----------|----------|----------|
| fixed gain | -36.3 dB | -47.5 dB | -55.1 dB |
| AGC | -57.1 dB | -63.8 dB | -67.1 dB |

The samples of the myo-electric and accelerometric signals are packed for a better efficiency of transmission. Each packet has a header defined by means of a protocol that has been developed for this specific application, in order to perform the temporal synchronization and the recovering of data flow in a sensor network. With the payload structure shown in Fig. 9, defined for ADC resolutions of up to 12 bits, and with the previously mentioned sample rates, the theoretical maximum number of nodes m operating on the same RF channel is 6, with an extra time slot available for retransmissions in case of errors. The actual limit depends on the particular RF environment and background noise, which affects the need and frequency of retransmissions, and is currently being investigated.

4 EXPERIMENTAL RESULTS

The prototype board was tested and used to acquire a sample EMG signal, reported in Fig. 1. Although proper shielding of the prototype was not employed due to the presence of auxiliary debugging and development connections, a quite good signal-to-noise ratio was achieved. Power consumption resulted in about 10 mA, with many power-saving optimizations that can still be implemented in the control software, thus making it possible to achieve a battery life of 5 to 10 hours of continuous operation out of a standard coin-size rechargeable Li-ion cell.

In order to show the effectiveness of the proposed AGC for EMG signal acquisition, some other experiments were also made. Figure 11 shows some of the results. It displays an EMG signal used as a reference, and the amplifier gains that were chosen by the AGC algorithm for each portion of the signal. The result was then quantized, and the quantized signal used to compute an estimate of the MAV. The MAV was smoothed with a fourth-order elliptical filter and the result shown in the same figure, and compared with that obtained from the unquantized version.

The results of the comparisons are shown in Table 1, which compares the errors made with different gain policies and different quantizer resolutions. As can easily be seen, the adoption of AGC permitted us to obtain an increase in the accuracy of the MAV

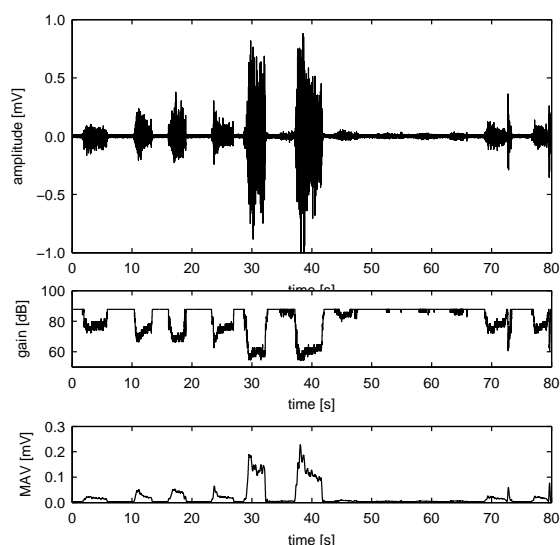


Figure 11: Operation of the AGC and resulting MAV estimate. From top to bottom: original EMG signal, optimal gain as selected by the AGC algorithm, post-quantizer MAV estimate.

estimation equivalent to more than two extra bits of resolution in the ADC, thus making it possible to use cheaper components without any serious degradation of the performance.

5 CONCLUSIONS

A complete wireless electromyographic system was developed, comprising a wearable sensor board, interacting with software running on a common PC for elaboration of the acquired data, and remote control of the acquisition circuitry for optimal system performance.

Moreover, the employed technology offers the capability of configuring reasonably large sensor networks for the analysis of several concurrent muscle fiber activities, also with base stations distributed in large area laboratories, and for example makes the analysis of running patients easier. The wireless EMG sensor makes the patients free of cumbersome wires and heavy transmitters and, as their movement are more natural, the resulting analysis is more adherent to reality. In comparison with other wireless technologies, these devices have a lower power consumption, a longer battery life, and the networks they realize can have a greater number of nodes and cover a longer distance.

In future works the microcontroller will be substituted by a low-cost DSP, embedding all the peripherals on it and augmenting the on-board signal process-

ing capabilities.

REFERENCES

- Berzuini, C., Figini, M. M., and Bernardinelli, L. (1985). Evaluation of the effectiveness of EMG parameters in the study of neurogenic diseases—a statistical approach using clinical and simulated data. *IEEE Transactions on Biomedical Engineering*, BME-32(1):15–27.
- Clancy, E. A. and Hogan, N. (1999). Probability density of the surface electromyogram and its relation to amplitude detectors. *IEEE Transactions on Biomedical Engineering*, 46(6).
- Jansen, B. H., Miller, V. H., Mavrofrides, D. C., and Jansen, C. W. S. (2003). Multidimensional EMG-based assessment of walking dynamics. *IEEE Transactions on Neural Systems and Rehabilitation Engineering*, 11(3).
- Kawakami, G., Nishida, Y., and Mizoguchi, H. (2007). In situ measurement of playing children by wireless wearable electromyography. In *Proc. IEEE Sensors Conference 2007*, Atlanta, GA, USA.
- Lemmerhirt, D. F., Staudacher, E. M., and Wise, K. D. (2006). A multitransducer microsystem for insect monitoring and control. *IEEE Transactions on Biomedical Engineering*, 53(10).
- Miyazawa, K., Ueno, A., Mori, H., Hoshino, H., and Noshiro, M. (2006). Development and evaluation of a wireless interface for inputting characters using laplacian EMG. In *Proc. 28th IEEE EMBS Annual International Conference*, New York City, NY, USA.
- Staudenmann, D., Kingma, I., Daffertshofer, A., Stegeman, D. F., and van Dieën, J. H. (2006). Improving EMG-based muscle force estimation by using a high-density EMG grid and principal component analysis. *IEEE Transactions on Biomedical Engineering*, 53(4).